Corona Discharges Glow on Trees under Thunderstorms

Enter authors here: P. J. McFarland[1], W. H. Brune[1], D. O. Miller[1] & J. M. Jenkins[1]

[1]Department of Meteorology & Atmospheric Science, The Pennsylvania State University, University Park, PA, 16802.

Corresponding author: Patrick J. McFarland (pmcfarland@psu.edu)

Key Points:

- A new ultraviolet-sensitive instrument has enabled the first direct observations of corona discharges on trees under thunderstorms.
- Corona discharges are transient in nature, often jumping from leaf to leaf and branch to branch but occur all across treetops.
- Ultraviolet emissions from corona discharges are directly proportional to currents flowing through trees under high voltage.

Abstract

Coronae, which are weak electrical discharges, have long been hypothesized to form on trees under thunderstorms, though never directly observed, characterized, or quantified. Using a newly developed instrument that measures ultraviolet emissions from coronae, the first direct observations and quantifications of coronae are presented for two trees under a thunderstorm in North Carolina. Coronae moved sporadically among leaves on every tree branch in a narrow field of view while the thunderstorm was directly overhead. Coronae emitted ~10^{11} photons at 260 nm, corresponding to electrical currents of ~1 μA, derived from unique measurements relating corona intensity to tree electrical current. Similar results across four additional storm intercepts from Florida to Pennsylvania give rise to a vision of swaths of scintillating corona glow as thunderstorms pass over forests. Such widespread coronae have implications for the removal of hydrocarbons emitted by trees, subtle tree leaf damage, and limited thunderstorm electrification.

Plain Language Summary

Most people know about lightning and the havoc it wreaks on forests. They do not know about the weak electrical glow, called a corona, that is thought to form on tree leaves under thunderstorms. Coronae may have been seen in total darkness, but their amount and behavior have never been documented. Here, we present the first observations of the ultraviolet glow from coronae on trees under thunderstorms. Coronae glowed on a sweetgum tree and a pine tree during a thunderstorm in North Carolina. It hopped among leaves and sometimes followed a branch as it swayed in the wind. Similar observations were made on other trees under four other thunderstorms from Florida to Pennsylvania. Our observations indicate that corona shimmer on the swath of trees beneath a thunderstorm. These coronae can alter air quality in forests, subtly damage leaves, and possibly give charge to overhead thunderstorms.

1 Introduction

Thunderstorms have been roiling over forests for eons. The most dramatic observed and studied effect is cloud-to-ground lightning and its ability to split trees asunder or to start forest fires (Fuquay et al., 1972). A lesser-known effect is the formation of coronae on tree leaves under thunderstorms. Coronae are weak electrical discharges, with temperatures only slightly above the surrounding air (Fridman et al., 2005), unlike lightning that raises air temperatures to tens of thousands of degrees (Uman, 1964). Yet coronae and their ultraviolet radiation produce extreme amounts of hydroxyl (OH), the atmosphere's main oxidizer (Brune et al., 2021; Jenkins et al., 2021; Jenkins et al., 2022), damage tree leaves (Rogers et al., 1984; Zaffanella & Deno, 1978; Miller & Kaufmann, 1978; Ovington, 1956; Repo et al., 2004), and potentially contribute charged particles to the thunderstorm cloud base (Malan and Schonland, 1951; Vonnegut et al., 1962; Helsdon et al., 2002; Masuelli et al., 1997).

A literature search found no documented direct observations of coronae on trees under thunderstorms, although coronae are one scientific explanation for the biblical burning bush (Sibley, 2009). Visible emissions of coronae are weak, even compared to that of a sliver moon, and they are therefore difficult to see with the human eye. While coronae formation under thunderstorms has been inferred by weaker-than-expected electric fields in forests when

thunderstorms are overhead (Standler & Winn, 1979; Soula et al., 1995; Chauzy & Raizonville, 1982; Toland & Vonnegut, 1978; Vonnegut & Rechnitzer, 1974), no direct measurement has ever been made of coronae quantity nor has coronae behavior ever been documented as the thunderstorm passes over a forest.

Here, we present the first direct observations of coronae and analyses of their behavior on a sweetgum and loblolly pine tree under a thunderstorm in North Carolina. These observations were made using a new solar-blind instrument that detects the ultraviolet (UV) radiation emitted by these weak discharges. The ability of this instrument to measure coronae was thoroughly tested under controlled conditions as well as deployed in the field. At Earth's surface, only electrical discharges, hot fires, or mercury lamps can produce the UV radiation to which this new instrument is sensitive (DeMore et al., 1997; Grum & Costa, 1976; Ding et al., 2025; Bergman, 2021). Hot fires and mercury lamps were absent during our observations, leaving only coronae as the source of measured UV signals.

2 Measurement and data analysis methods

2.1 Mobile Corona Measurement System

For this research, we developed a multi-component mobile instrument capable of measuring coronae on treetops and atmospheric properties that can influence their formation (Fig. S1). The component most sensitive to coronae UV radiation is the Corona Observing Telescope System (COTS; Fig. S2), a 25-cm diameter telescope (Orion 10" f4.0 Newtonian Astrograph model # 10271) that focuses the UV radiation onto a solar-blind UV camera sensitive to wavelengths between 255-273 nm (proprietary to OFiL Systems, LTD). The COTS UV camera has a field of view of ~2.5° by 1.5°, video output of 445440 pixels in a 928×480 matrix, and a frame rate of 30 frames s^{-1}. A few percent of the beam exiting the telescope is focused on a visible camera (Watec WAT-221S) with a similar field of view. The COTS telescope is mounted vertically in a research vehicle and can view in any direction through a periscope containing two ¼-wave flat mirrors (Precision Optical) mounted on the vehicle roof. The weatherproof periscope window consists of 0.05-mm thick Teflon FEP film.

In addition to the COTS UV camera, the vehicle is equipped with a GPS (VK-162 G-Mouse USB GPS), electric field mill (EFM; Boltek EFM-100), weather station (SwitchDocLabs SkyWeather2), and laser rangefinder (Nikon ProStaff 1000). The GPS provides location information as well as time syncing across all instruments. The EFM, mounted on top of the vehicle, measures the strength and polarity of the vertical component of the electric field relative to the vehicle roof. Note the EFM yields a relative measurement, not the actual electric field at the ground or the treetop, but it is useful for determining the degree of electrification present in the overhead thunderstorm and for identifying nearby lightning strikes. The weather station is primarily used to measure ambient temperature, pressure, relative humidity, and rainfall rate, all of which are necessary to calculate the radiative effects of observed coronae.

Finally, the laser rangefinder is used to determine the distance between the vehicle and the tree being examined.

2.2 COTS Sensitivity to Corona Radiation

To quantify the UV radiation emitted by coronae, connect with their associated current flows, and enable estimation of their chemical implications, the COTS is calibrated using a National Institute of Standards and Technology (NIST)-traceable deuterium lamp (StellarNet SL3). This lamp was placed 25 m from the COTS periscope, a distance typical for coronae measurements at the tops of ~20 m tall trees under thunderstorms. The COTS UV camera has also been tested against coronae on small spruce and maple trees in artificial electric fields, as described below.

Two calibration tests were performed. First, the deuterium lamp shone into the COTS periscope, overfilling it by a factor of ~100. Second, an antireflection-coated lens (50 mm diameter, 100 mm focal length, 98% transmissivity) was placed in front of the deuterium lamp, focusing the beam to almost the same area as the telescope primary mirror, the COTS limiting aperture. The spectral irradiance, F(λ), emitted by the lamp is ~0.23 W m^{-2} nm^{-1} between 255-273 nm, the full width half maximum (FWHM) of the COTS UV camera. The irradiance was reduced with a 0.53 mm diameter aperture placed at the lamp calibration plane and a neutral density filter (9×10^{-5} transmissivity). As a result, ~1.1×10^{8} photons s^{-1} were propagated through the optical system and available for COTS detection.

The COTS UV camera detects individual photons, which appear as illuminated white pixels on a black background in the video frames. Dividing the photons s^{-1} entering the COTS periscope by the number of illuminated pixels s^{-1} recorded, each illuminated pixel is equivalent to ~4.5×10^{4} photons $pixel^{-1}$, or a detection efficiency of $(2.2\pm0.77)\times10^{-5}$ pixels $photon^{-1}$, 35% uncertainty at 68% confidence. To apply this calibration at other distances, we divide this photon equivalent signal by the steradians subtended by the COTS at 25 m, which is 8.1×10^{-5} sr, resulting in 5.5×10^{8} photon sr^{-1} $pixel^{-1}$. For isotropic coronae radiation, an illuminated UV pixel corresponds to the total coronae emission of 7.0×10^{9} photons.

For coronae that are more episodic, it is convenient to think in terms of the number of illuminated pixels per video frame (1/30 s). If a corona discharge lasts for more than one frame, the total photons emitted during a corona cluster is the sum of illuminated pixels per frame for all the frames within that corona cluster.

2.3 COTS Data Collection and Processing

A digital video recorder (Speco Technologies H6HRL) gathers and saves video feeds from the cameras, while a laptop collects and saves the electric field, weather station, and GPS location information. Time syncing across all instruments is maintained by the BKtTimeSync application (https://www.maniaradio.it/en/bkttimesync.html) using the GPS time as standard.

Videos and data are collected for most of the storm, typically from the first rain to a few minutes before rain cessation.

The video analysis consists of several steps, which are explained in more detail in the Supporting Information (Text S1). First, frames with illuminated pixels are identified. Often, several illuminated pixels form a contiguous bundle termed a UV signal. Second, illuminated pixels are filtered by their distance to the tree in the corresponding visible frame, rejecting illuminated pixels far from the tree that are unlikely from UV radiation on tree leaves (Fig. S3). Third, a Density Based Spatial Clustering Algorithm with Noise (DBSCAN; Schubert et al., 2017; Fuchs et al., 2016) finds groupings called potential corona clusters that are at least a factor of two greater than the average COTS UV camera background noise of 0.31 pixels frame^{-1}. For a potential corona cluster to be identified, two criteria must be satisfied: at least 1 illuminated UV pixel must occur in 4 distinct frames, and frames containing illuminated UV pixels must be separated by no more than 35 frames, or 1.16 s. These thresholds were chosen because they maximized the real corona cluster to noise cluster ratio (Figs. S3-S4) as determined by measurements under thunderstorms compared to cases when the COTS UV camera was left capped. When the DBSCAN algorithm is applied to the noise data, no noise clusters appear (Please see Supporting Information Text S1 for more details on the choice of these thresholds.)

Each potential corona cluster identified by the DBSCAN algorithm is manually checked and sorted into two categories: coronae only or coronae and lightning. Coronae-only clusters are manually confirmed when there are repeated illuminated UV pixels around the tree. An especially telling sign is when the illuminated UV pixels track with a leaf or branch as it sways in the wind, as is often the case (Movie S1). Coronae and lightning clusters, on the other hand, illuminate most of the COTS UV pixels for several frames. Lightning is further confirmed by corresponding spikes recorded by the EFM.

While lightning UV radiation interferes with direct coronae observations, it is very likely that some coronae occur at the same time, since current flows through trees were measured to be largest around times of nearby lightning (Standler & Winn, 1979). Since lightning appears as a random, uniform interference, we filter it out by comparing the density of illuminated pixels away from the tree (illuminated pixels away from tree ÷ total pixels away from tree) to those within the tree. Any leftover signal within the tree after subtracting off the lightning signal is from coronae. Under a minimal rainfall rate of ~3 mm hr^{-1}, the UV reflectivity of rain was determined to be much greater than the UV reflectivity of the tree branch itself. As a result, it is unlikely UV signals within the tree at times of lightning are from lightning reflection. For the 27 June 2024 case presented here, the DBSCAN algorithm identified 49 potential corona clusters. Twenty-eight, or 57% were found to be from coronae only while the remaining 21, or 43% contained lightning.

In identifying potential corona clusters, it is assumed that a single corona discharge persists from the first illuminated UV pixel to the last, albeit at low signal rates with statistical gaps. Alternatively, it is possible, though unlikely, that each illuminated UV pixel is a brief, unique corona, and there exists a multitude of these short duration discharges that cannot be

distinguished from noise on the COTS UV camera (Text S1). No attempt to discern between these two possibilities is made in this study, as the clustering assumption was made strictly for the purpose of filtering noise. However, by removing all noise, up to 25% of potential corona clusters were removed as well (Text S1). Thus, the prevalence of coronae reported here is an underrepresentation by as much as a factor of ~1.25. When these uncertainties are combined with the above calibration uncertainty, the COTS sensitivity may be an underestimate by a factor of 1.35 to an overestimate by a factor of 1.6. Thus, the total COTS calibration is 5.5×10^{8} photon sr^{-1} $pixel^{-1}$, with a range of $(3.4\text{-}7.7)\times10^{8}$ photon sr^{-1} $pixel^{-1}$, 68% confidence.

2.4 COTS Signals to Corona Currents

This work, for the first time, has directly linked the current measured through small trees to coronae intensity determined by their UV emissions. For these experiments, the COTS UV camera observed ~1 m tall Spruce and Maple trees in plastic pots that were subjected to enhanced electric fields. The treetops were placed 15 cm beneath a 66 cm by 61 cm aluminum plate charged with a high voltage power supply (Information Unlimited HV350REG) rated to $\pm$35 kV. A grounded metal ring below the charged plate encircled but did not touch the tree 70 cm below the top plate, creating electric fields as high as 40 kV m^{-1}. To minimize leakage current, the trees were raised 2.5 cm from the laboratory floor by four Teflon rings (Text S2). Corona current was measured by a picoammeter (Keithley 6485) between a copper plate in the soil of the potted tree and an electrical ground.

3 Results

3.1 Relationships between electric field, current, and corona UV signals

Across all voltages tested for both the Spruce and Maple trees, both the quadratic curve derived by Cobine (1941) and Warburg (1899) and the cubic curve derived by Jhawar & Chalmers (1967) fit the applied voltage to measured current relationship, with $R^2 > 0.9$. The cubic curve consistently yielded slightly greater correlations (Fig. S5), in agreement with Standler & Winn (1979) who similarly found both the cubic and quadratic relationships to be adequate, though the cubic relationship fit the extreme values better.

As each tree was subjected to high voltages, the COTS UV camera measured corona UV signals from 12 m away. COTS UV signals linearly increased with measured current independent of tree type, electric field, and hydraulic conductance (Text S2-S3; Fig. S6-S7). When the overhead plate was positively charged, negative point-like coronae formed on the trees (Dordizadeh et al., 2016; Jenkins et al., 2022), and measured currents were proportional to COTS count rates by a factor of $5.07\text{x}10^{-2}$ µA s $pixel^{-1}$ with an R^2 of 0.98 (Fig. S6). Conversely, when the plate was negatively charged, positive streamer-like coronae formed (Dordizadeh et al., 2016; Jenkins et al., 2022), and COTS count rates were related to measured currents by a factor of 0.192 µA s $pixel^{-1}$ with an R^2 of 0.87. As the polarity of coronae can be determined from EFM polarity (Soula et al., 1995), observations of coronae on trees under thunderstorms

also enable estimation of current flowing through the examined portion of the tree, a long-sought quantity (Jhawar & Chalmers, 1967).

3.2 Measurements of Coronae on two trees in North Carolina

On 27 June 2024, the COTS vehicle was in a large, open parking lot at the northern extreme of the University of North Carolina Pembroke campus examining the top branches of a sweetgum tree 32 m away (Fig. S8a). The sweetgum tree was observed for about 1.5 hours; then, the COTS vehicle moved ~40 m to examine a long needle loblolly pine tree (Fig. S8b) 28 m away for ~20 minutes under the trailing stratiform precipitation region of the storm.

During the ~1.5 hours observing the sweetgum tree, 859 UV signals, contiguous bundles of several illuminated pixels, grouped into 41 DBSCAN corona clusters were observed on three branches, the only branches examined on this tree (Fig. 1a). 306 UV signals and 21 DBSCAN corona clusters were from coronae signals alone while the remaining 553 UV signals and 20 DBSCAN clusters comprise coronae signal at times of coincident lightning. All clusters lasted between 0.13 and 3.33 s and behaved sporadically by hopping from leaf to leaf and sometimes repeating on the same leaf. One corona observed on the sweetgum tree is described in detail in the Supporting Information (Text S4; Fig. S9; Movie S1). Such sporadic signal is characteristic of even laboratory coronae on a tree under a constant electric field, as documented previously (Aubrecht et al., 1999) and confirmed by our laboratory studies (Text S5; Fig. S10), in which the coronae are seen sporadically hopping from leaf to leaf among five different locations along the

top canopy of the small, potted Maple tree. Under a highly heterogeneous charged thunderstorm, the sporadic nature of coronae is only further exacerbated.

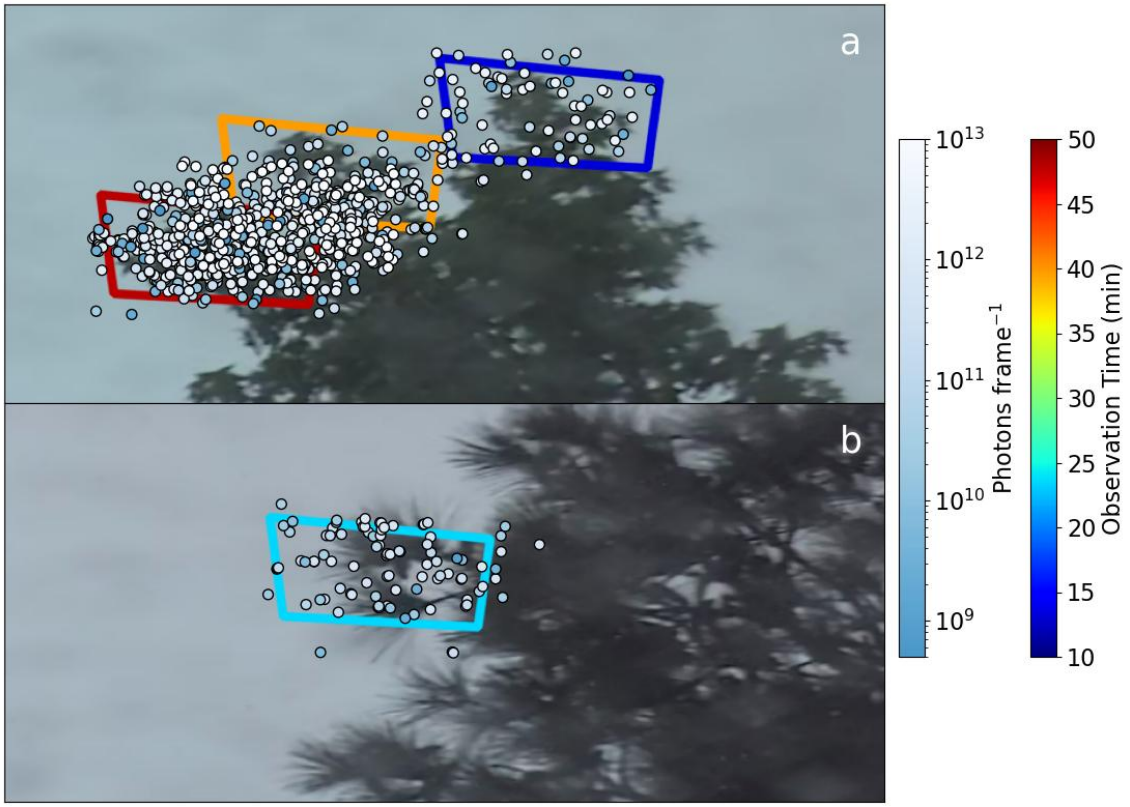

Figure 1. Corona UV signals observed under a thunderstorm on 27 June 2024. (a) Approximate location of all 859 corona UV signals observed during the ~1.5-hour observation period on a sweetgum tree. Each corona UV signal is colored by the number of total isotropic UV photons between 255 and 273 nm emitted by the corona discharge, as estimated from the illuminated pixels observed in that frame. The boxes depict the COTS UV camera field of view, and the colors indicate the observation time for the branch within each box. (b) As in (a), but for all 93 corona UV signals observed during the ~20-minute observation period on a loblolly pine tree. Locations of boxes and corona UV signals are only approximate because the wind blew the branches in and out of the COTS field of view. Note a corona UV signal is defined as a contiguous bundle of several illuminated pixels.

Using the photon calibration (section 2.2), UV photon fluxes of 10^0 to 10^4 photons cm^{-2} frame^{-1} were observed for individual frames containing UV signals. For isotropic corona discharge radiation, this photon flux translates to a total emission of 10^8 to 10^{12} photons frame^{-1}. The total corona UV radiation in the wavelength band below 300 nm is about seven times greater than the narrow wavelength band of COTS sensitivity (Text S6). Thus, leaves and the surrounding air are exposed to ~10^{10} to 10^{14} energetic UV photons from a 1-second duration corona discharge. Because the ~10^{14} photons cm^{-2} s^{-1} of solar UV in the COTS wavelength band

is completely blocked by the stratospheric ozone layer, coronae, lightning, and fire are the only natural sources for tree leaf exposure to such energetic UV radiation.

Different branches of the sweetgum tree were observed for different durations during the thunderstorm (Fig. 1a). At least some of the leftmost (red box), middle (orange box), and rightmost (blue box) branches were observed for 48 minutes, (65% of the observation time), 40 minutes (54%), and 13 minutes (18%), respectively. These observation times closely align with the fractions of corona UV signals observed, as the leftmost, middle, and rightmost branches contained 61%, 51%, and 12% of the corona UV signals. When normalized by observation time, coronae therefore formed uniformly across all three branches examined on this tree.

After ~1.5 hours of examining the three branches at the sweetgum treetop, the COTS vehicle moved 40 m to view the top branch of a loblolly pine tree. In ~20 minutes, 93 corona UV signals were detected and grouped into 8 DBSCAN coronae clusters (Fig. 1b). 68 UV signals and 7 DBSCAN clusters were from coronae signals alone while the remaining 25 UV signals and 1 DBSCAN cluster occurred coincidently with lightning. Like the sweetgum tree corona clusters, the loblolly pine corona clusters persisted between 1.3 and 2.6 s and emitted on the order of 10^8 to 10^{11} photons frame^{-1}. Coronae were also measured at similar frequencies as on the three branches of the sweetgum tree. Thus, observed coronae were nearly identical on the sweetgum and loblolly pine trees despite vastly different leaf morphologies and storm intensities when being observed.

Measured coronae corresponded to an estimated current flow through the individual tree branches on the order of 1 μA (Fig. 2c). Only one study has directly measured the coronae current through trees under electrically isolated thunderstorms, though without any direct measure of the coronae themselves (Standler & Winn, 1979). In their experiments, Standler & Winn (1979) measured currents on the order of 10^{-1} μA. However, their measurements were reported only when “the electric field was not changing rapidly with time.” Conversely, 43% of estimated coronae currents derived here occurred coincidently with lightning and therefore rapid changes in the electric field. At these times, it is unsurprising to expect greater estimated

current pulses. The three largest estimated current pulses, -53 µA at 19:37:46, -33 µA at 20:04:21 UTC and -11 µA at 19:17:44 UTC, were coincident with lightning (Fig. 2b-c).

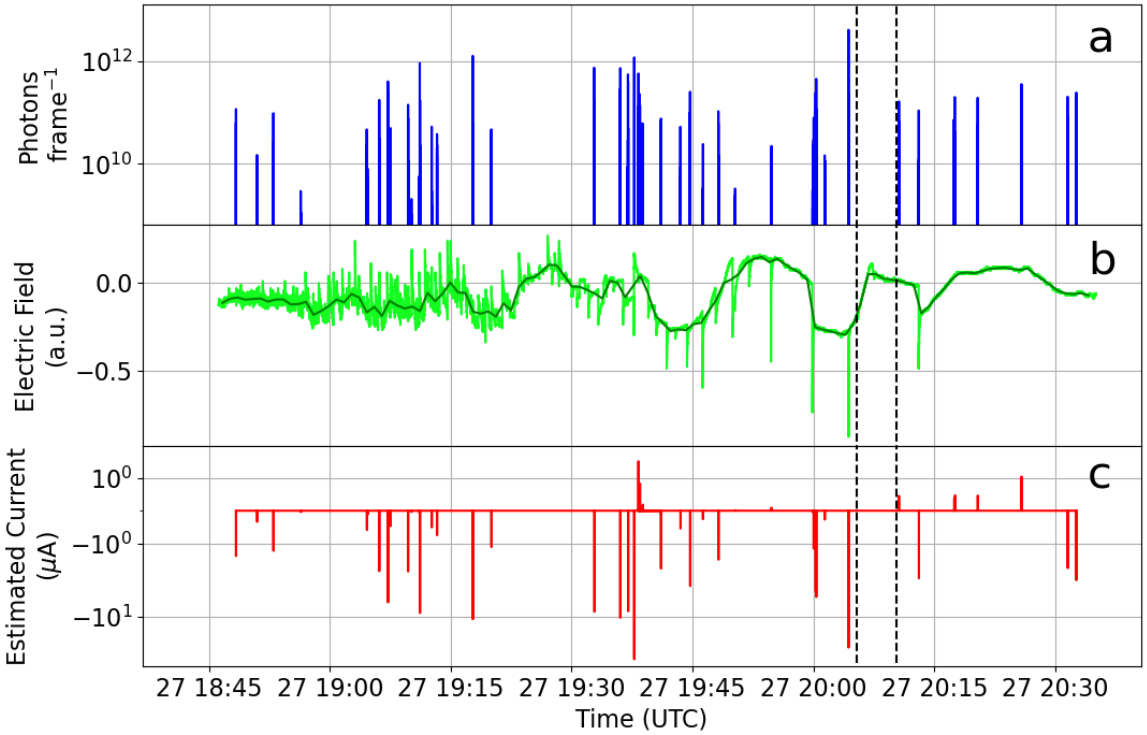

Figure 2. Time-series of coronae UV emissions, electric field, and derived coronae current throughout the 27 June 2024 case. The panels are (a) estimated total coronae photon emission from observed coronae UV signals; (b) uncalibrated electric field (light green) and 1-minute median electric field (dark green) measured by the EFM on the roof of the COTS vehicle; and (c) derived coronae current for the portion of the tree being examined. The dashed black vertical lines denote the time the COTS vehicle switched from examining the sweetgum to loblolly pine tree.

The present study extends the work of Standler & Winn (1979) to currents flowing through branches of mature, ~20 m-tall trees under thunderstorms, and provides the first direct evidence of coronae existence that was only implied in the former. Despite the many differences between the two studies, similar coronae currents are reported. Standler & Winn (1979) reported a maximum coronae current of 600 nA through their small ~2 m-tall trees. Coronae currents on that same order were derived under relatively steady overhead electric fields between 20:01 and 20:03 UTC, and 20:17 and 20:21 UTC (Fig. 2). In total, 47% of derived coronae currents were less than 600 nA.

On the sweetgum tree, three spans of frequently observed coronae are separated by two periods relatively devoid of coronae (Fig. 2a). The first of these intensive coronae observations persisted from 19:04 to 19:20 UTC, preceded by a few coronae observed as the leading edge of the thunderstorm passed overhead. During this ~15-minute period, the COTS vehicle was under the thunderstorm core, with rainfall rates exceeding 40 mm hr^{-1} and EFM-

derived lightning flash rates greater than 5 min^{-1}. Then, from 19:20 to 19:32 UTC, no coronae were observed as the electric field reversed polarity, becoming positive.

The second and most intensive span of frequent coronae observations occurred between 19:32 and 19:48 UTC. During this time, the COTS was beneath the trailing lighter-precipitating stratiform region of the storm between two convective cores: the one that passed overhead during the previous intensive coronae observation span that was centered ~33 km east-southeast, and a second centered about 28 km southwest traveling tangent to the COTS location. The charge structure in this stratiform region of the storm was therefore likely highly heterogeneous (Dye & Bansemer 2019; House, 2014), as coronae of both polarities were recorded during this period (Fig. 2c).

This second span of intensive coronae observation again terminated as the electric field reversed polarity (Fig. 2b). Two coronae were detected while the electric field was positive, though both occurred coincidently with lightning. A positive overhead electric field induces a negative charge in the tree. Negative coronae require similar electric fields to initiate as positive coronae (Lowke & D'Alessandro, 2003; English, 1948), yet they appear more luminous in the UV (Text S2), making them easier to detect than their positive counterparts. That no coronae were observed at these times must therefore indicate the electric field surrounding the tree never reached the necessary threshold to initiate negative coronae. While greater electric field magnitudes were recorded at these times devoid of coronae than at several periods with frequent coronae, the measured electric field is uncalibrated, relative to the roof of the COTS van, and is not representative of the field at treetop (Soula et al., 1995; Standler & Winn, 1979).

The third and final span of intensive coronae observations on the sweetgum tree occurred from 20:00 to 20:04 UTC (Fig. 2a). The electric field measured large, negative, stable values for the entirety of this period. Overhead radar reflectivity increased to ~36 dBZ from ~30 dBZ during the second span of intensive coronae observations and rainfall rates similarly increased to ~4 mm hr^{-1} from ~2 mm hr^{-1}, indicative of a decaying thunderstorm cell behind the main convective line. After 20:04 UTC, our decision to switch trees to examine the loblolly pine may have prematurely terminated this span of frequent coronae observation, though the electric field polarity reversal nearly coincided with this decision.

On the loblolly pine tree, coronae were measured every few minutes under a positive electric field (Fig. 2). Overhead radar reflectivity values remained greater than 35 dBZ and rainfall rates persisted near 4 mm hr^{-1} for the duration of loblolly pine observations, as the COTS vehicle remained in the trailing stratiform precipitation region. Of all tree leaves tested in our laboratory experiments, coronae initiated at the lowest voltage on spruce, which share a similar morphology, albeit with shorter needles, to the loblolly pine (Jenkins et al., 2022). This low onset voltage is attributable to the enhancement of the electric field around the sharp

points on the needles (Moore et al., 2000). Thus, coronae were likely able to form on the loblolly pine tree under electric fields weaker than those necessary for the sweetgum tree.

4 Discussion

In addition to the thunderstorm case presented in detail above, sporadic coronae that hopped among leaves and branches have been measured under at least four additional thunderstorms on at least four additional tree types from Florida to Pennsylvania (Table S1). For all cases, similar photon emission rates and currents were derived from ubiquitous coronae under both the thunderstorm convective core and electrified trailing stratiform region.

The transient nature of the UV signals in corona clusters on trees results from several factors. First, even under a constant electric field in the laboratory, coronae were found to hop from one location to another (Text S5; Fig. S10). Thus, some degree of transience is an intrinsic trait of corona discharges. Second, the wind can impact coronae intensity and current flow (Large & Pierce, 1957; Chapman, 1970; 1977) by reorienting leaves so that their fine points are oriented upward or by creating fluctuations in the electric field enhancement around the points. A computer simulation of a stem of locust leaves beneath a charged plate demonstrates that the leaves pointed toward the charged plate had highly enhanced electric fields on their tips while leaves pointed away from the charged plate did not (Text S7; Fig. S11). Third, the current to form coronae must flow up through the tree and leaves, which depends on the hydraulic conductance, or flow of water through the tree (Text S3; Fig. S7; Ganthaler et al., 2019; Nadler et al., 2008; Bucci et al., 2003; Flexas et al., 2003; Afzal et al., 2017; Mancuso, 1999). Variations in hydraulic conductance contribute to coronae transience (Aubrecht et al., 1999; 2000). Note that most of this transience is specific to plants, further demonstrating that metal rods are poor analogs for the behavior of coronae on trees under thunderstorms (Aubrecht et al., 1999).

Several factors could cause the number of coronae observed by the COTS to be an underestimate. First, some corona UV signals occurring within the COTS field of view may have been blocked by other leaves between the COTS and corona location. This blockage is estimated to be no more than 20% since corona UV signals tend to form on the uppermost leaves and extend away from the tree (Fig. S10). Second, some coronae were possibly below the detection limit of the COTS UV camera (Text S2). However, no coronae were within a factor of two of the detection limit and only 8% were within a factor of three. The dearth of coronae near the detection limit implies few to none exist below it, making it unlikely to be a substantial factor. Third, as stated previously in section 2.3 and Text S1, an estimated 25% of corona UV signals were filtered out by the clustering method, though this factor is already accounted for in the calibration. Thus, coronae frequency could be as much as 20% greater than presented here.

Derived currents from observed coronae spanned several orders of magnitude, with 53% exceeding 600 nA, the maximum current measured by Standler & Winn (1979), attributable to several factors. First, Standler & Winn (1979) measured the current flow through a ring of six immature trees less than 2 m tall. Conversely, our derived coronae currents were from mature ~20 m tall trees. Second, most of the current measurements reported by Standler

& Winn (1979) were taken under a dry thunderstorm, whereas our measurements were taken during steady rain sometimes exceeding 40 mm hr^{-1}. The presence of water on tree leaves is known to increase corona UV emission, and therefore current, by 30-40% (Jenkins et al., 2022). Third, much larger currents than those reported by Standler & Winn (1979) were measured in our laboratory experiments (Text S2; Fig. S5). The trees in our laboratory experiments were subjected to maximum electric fields of ~40 kV m^{-1}, similar to those measured at elevations typical of mature treetops (Soula et al., 1995; Chauzy & Raizonville, 1982). Conversely, the electric fields around the immature trees in Standler & Winn (1979) did not exceed 10 kV m^{-1}.

In summary, this research is unique in several ways: the first detection of UV emissions from coronae on trees under thunderstorms; the first observations and descriptions of the transient, leaf-hopping behavior of coronae on multiple branches of several trees under thunderstorms; and the first development of equations relating coronae UV emissions, and thus coronae intensity, with electrical current flowing through electrically isolated trees under controlled direct-current high voltages. Future studies will be necessary to establish a universal relationship between electrical current flowing through trees with observed coronae UV emissions, and to directly link these currents and coronae UV emissions to electric fields at treetop for a wide range of trees and forest environments.

5 Implications

Everywhere along the tops of trees and every tree observed under thunderstorms had similar amounts of coronae, implying that favorable leaves on branches across the treetop of every tree under the electrified thunderstorm had similar amounts of coronae. While coronae frequency and intensity depend on the electric field, coronae will form on the most favorable leaves as long as an electrified thunderstorm core or anvil is overhead. This ubiquity of observed coronae gives rise to a vision of a swath of scintillating corona glow as the electrified thunderstorm passes over a forest.

Potential coronae impacts are therefore widespread and merit further investigation. For instance, Jenkins et al. (2022) estimated coronae produced ~10^{17}-10^{18} molecules of the hydroxyl radical (OH) surrounding a treetop during a thunderstorm, at least three orders of magnitude greater than all other well-known OH production mechanisms that surround the treetop combined. With these first-ever measurements of corona on trees under thunderstorms, more accurate estimates of corona-generated OH are possible.

Coronae also have potentially substantial impacts on trees, especially in regions of frequent thunderstorms. The fibrous fine leaf tips that form coronae become visibly burnt in as little as a few seconds for applied voltages of ~10 kV, initiating leaf damage (Jenkins et al., 2022). Additionally, coronae current flows are potentially much greater than those derived from observed coronae (Fig. 2c), as the COTS only viewed a small ~1 m^2 portion of the treetop and the derived current is reported only from the branch in the COTS field of view. If individual leaves scattered across the ~100 m^2 treetop of the sweetgum tree glowed with coronae, current flows on the order of hundreds of microamps would be expected. Repeated exposure to such surges of coronae current through the tree could kill the upper tree branches, as would

happen if the tree forms an upward lightning leader that fails to attach to the downward stepped leader of a cloud-to-ground lightning flash (Krider and Ladd, 1975). These first coronae measurements contribute to emerging studies of the impacts of coronae and electrical discharges on trees (Gora et al., 2025).

Quantification of corona extent and intensity will also refine estimates on charged particles emitted by coronae and their downstream impacts, including on thunderstorm electrification. While unlikely to be a significant source of charged particles (Helsdon et al., 2002; Masuelli et al., 1997), those emitted by coronae could possibly stimulate weak discharges near cloud base similar to the blue corona discharges recently discovered near cloud top (Chanrion et al., 2017; Husbjerg et al., 2022).

Coronae on trees under thunderstorms have been mentioned in the science literature for almost a century. Not until now, however, have coronae been directly observed, their behavior described, their UV emissions quantified, and their relationship with current demonstrated. The impacts these coronae have on atmospheric chemistry, forest ecology, health, and evolution, and thunderstorm electrification must be re-evaluated and understood, especially as thunderstorms, and therefore coronae, increase in a warming climate.

Acknowledgments

This work was supported by National Science Foundation (NSF) grant AGS-2323203 awarded to W. H. B. We thank Eran Fritch and OFiL Systems, LTD for taking an interest in this research and providing us with their solar-blind ultraviolet cameras. Two undergraduate students, Sophia Kennelly and Ethan Myers, aided in the laboratory and calibration experiments. We thank them for their help. We also thank the University of North Carolina Pembroke for allowing the use of their facilities. We thank the three anonymous reviewers for their useful comments.

Conflict of Interest Statement

The authors have no conflicts of interest to disclose.

Open Research

Corona UV signal data are available at McFarland et al. (2025).

References

Afzal, A., Duiker, S. W., Watson, J. E. & Luthe, D. (2017), Leaf thickness and electrical capacitance as measures of plant water status. *Transactions of the ASABE* 60(4), 1063-1074.

Aubrecht, L., Koller, J. & Stanek, Z. (2000), Onset voltages of atmospheric corona discharges on plants, *Czech. J. Phys.,* 50(313).

Aubrecht, L., Koller, J. & Zahoranova, A. (1999), Trichel pulses in negative corona discharge on trees, *J. Phys. D: Appl. Phys.,* 32(18), L87.

Bergman, R. S. (2021), Germicidal UV sources and systems. *Photochem. Photobiol.,* 97, 466-470.

Brune, W. H., McFarland, P. J., Bruning, E. C., Waugh, S., MacGorman, D., Miller, D. O., Jenkins, J. M., Ren, X., Mao, J. & Peischl, J. (2021), Extreme oxidant amounts produced by lightning in storm clouds. *Science* 372(6543), 711-715.

Bucci, S. J., Scholz, F. G., Goldstein, G., Meinzer, F. C. & Sternberg, L. D. S. L. (2003), Dynamic changes in hydraulic conductivity in petioles of two savannah tree species: Factors and mechanisms contributing to the refilling of embolized vessels. *Plant, Cell, & Environment* 26, 1633-1645.

Chanrion, O., Neubert, T., Mogensen, A., Yair, Y., Stendel, M., Singh, R. & Singh, D. (2017), Profuse activity of blue electrical discharges at the tops of thunderstorms. *Geophys. Res. Lett.* 44, 496-503.

Chapman, S. (1970), Corona point current in wind. *J. Geophys. Res.* 75(12), 2165-2169.

Chapman, S. (1977), The magnitude of corona point discharge current. *J. Atmos. Sci.* 34(11), 1801-1809.

Chauzy, S. & Raizonville, P. (1982), Space charge layers created by coronae at ground level below thunderclouds: Measurement and modeling. *J. Geophys. Res.* 84(C4), 3143-3148.

Chen, J. & Davidson, J. H. (2002), Electron density and energy distributions in the positive DC corona: Interpretation for corona-enhanced chemical reactions. *Plasma Chemistry and Plasma Processing* 22, 199-224.

Cobine, J. D. *Gaseous Conductors* (McGaw-Hill, 1941).

DeMore, W. B., Sander, S. P., Golden, D. M., Hampson, R. F., Kurylo, M. J., Howard, C. J., Ravishankara, A. R., Kolb, C. E. & Molina, M. J. (1997), Chemical kinetics and photochemical data for use in stratospheric modeling evaluation number 12, *NASA JPL Publication 97-4*.

Ding, Z., Rakov, V. A., Zhu, Y., Chen, S., & Kereszy, I. (2025), Positive and negative lightning leaders imaged in UV and visible ranges, *Geophys. Res. Lett.,* 52, e2024GL113689.

Dordizadeh, P., Adamiak, K. & Castle, G. S. P. (2016), Study of the impact of photoionization on negative and positive needle-plane corona discharge in atmospheric air. *Plasma Sources Science and Technology* 25(6), 065009.

Dye, J. E. & Bansemer A. (2019), A. Electrification in mesoscale updrafts of deep stratiform and anvil clouds in Florida. *J. Geophys. Res. Atmos.* 124, 1021-1049.

English, W. D. (1948), Positive and negative point-to-plane corona in air. *Phys. Rev.* 74, 170.

Flexas, J., Scoffoni, C., Gago, J. & Sack, L. (2013), Leaf mesophyll conductance and leaf hydraulic conductance: An introduction to their measurement and coordination. *Journal of Experimental Botany* 64(13), 3965-3981.

Fridman, A., Chirokov, A. & Gutsol, A. (2005), Non-thermal atmospheric pressure discharges, *J. Phys. D: Appl. Phys.,* 38.

Fuchs, B., Bruning, E. C., Rutledge, S. A., Carey, L. D., Krehbiel, P. R. & Rison, W. (2016), Climatological analyses of LMA data with an open-source lightning flash-clustering algorithm. *J. Geophys. Res. Atmos.* 121(14), 8625-8648.

Fuquay, D. M., Taylor, A. R., Hawe, R. G. & Schmid Jr., C. W. (1972), Lightning discharges that caused forest fires. *J. Geophys. Res.* 77(12), 2156-2158.

Ganthaler, A., Sailer, J., Bär, A., Losso, A. & Mayr, S. (2019), Noninvasive analysis of tree stems by electrical resistivity tomography: Unraveling the effects of temperature, water status, and electrode installation. *Front. Plant Sci.* 10.

Gora, E. M., Muller-Landau, H. C., Cushman, K. C., Richards, J. H., Bitzer, P. M., Burchfield, J. C., Navárez, P. & Yanoviak, S. P. (2025), How some tropical trees benefit from being struck by lightning: Evidence for *Dipteryx olifera* and other large-statured trees, *New Phytol.* 246, 1554-1566.

Grum, F. & Costa, L. F. (1976), Spectral emission of corona discharges, Applied Optics, 15, 76-79.

Helsdon Jr, H. J., Gattaleeradapan, S., Farley, R. D. & Waits, C. C. (2002), An examination of the convective charging hypothesis: Charge structure, electric fields, and maxwell currents. *J. Geophys. Res.* 107(D22), 4630.

House Jr, R. A. *Cloud dynamics* (Elsevier, ed. 2, 2014).

Husbjerg, L. S., Neubert, T., Chanrion, O., Dimitriadou, K., Li, D., Stendel, M., Kaas, E., Ostgaard, N. & Reglero, V. (2022), Observations of blue corona discharges in thunderclouds. *Geophys. Res. Lett.* 49, e2022GL099064.

Jenkins, J. M., Brune, W. H., & Miller, D. O. (2021), Electrical discharges produce prodigious amounts of hydroxyl and hydroperoxyl radicals. *J. Geophys. Res. Atmos.* 126, e2021JD034557.

Jenkins, J. M., Olson, G. A., McFarland, P. J., Miller, D. O. & Brune, W. H. (2022), Prodigious amounts of hydrogen oxides generated by corona discharges on tree leaves. *J. Geophys. Res. Atmos.* 127, e2022JD036761.

Jhawar, D. S. & Chalmers, J. A. (1967), Point-discharge currents through small trees in artificial fields. *Journal of Atmospheric and Terrestrial Physics* 29(11), 1459-1463.

Krider, E. P. & Ladd, C. G. (1975), Upward streamers in lightning discharges to mountainous terrain. *Weather* 30, 77-81.

Large, M. I. & Pierce, E. T. (1957), The dependence of point-discharge currents on wind as examined by a new experimental approach. *Journal of Atmospheric and Terrestrial Physics* 10(5-6), 251-257.

Lowke, J. J. & D'Alessandro, F. (2003), Onset corona fields and electrical breakdown criteria, *J. Phys. D: Appl. Phys.* 36, 2673.

Luque, A., Ratushnaya, V. & Ebert, U. (2008), Positive and negative streamers in ambient air: Modeling evolution and velocities. *J. Phys. D: Appl. Phys.* 41(23).

Malan, D. J. & Schonland, B. F. J. (1951), The distribution of electricity in thunderclouds. *Proc. R. Soc. Lond. A* 209, 158-177.

Mancuso, S. (1999), Seasonal dynamics of electrical impedance parameters in shoots and leaves related to rooting ability of olive (olea europea) cuttings. *Tree Physiology* 19(2), 95-101.

Masuelli, S., Scavuzzo, C. M. & Caranti, G. M. (1997), Convective electrification of clouds: A numerical study. *J. Geophys. Res.* 102(D10), 11049-11059.

McFarland, P. J., Brune, W. H., Miller, D. O., & Jenkins, J. M. (2025). Corona Discharges Glow on Trees Under Thunderstorms [Dataset]. Penn State Data Commons. https://doi.org/10.26208/9CZM-6Z29.

Miller, M. W. & Kaufman, G. E. (1978), High voltage overhead. *Environment: Science and Policy for Sustainable Development* 20(1), 6-36.

Moore, C. B., Rison, W., Mathis, J. & Aulich, G. (2000), Lightning rod improvement studies. *J. Appl. Meteor. Climo.* 39, 593-609.

Nadler, A., Raveh, E., Yermiyahu, U., Lado, M., Nasser, A., Barak, M. & Green, S. (2008), Detecting water stress in trees using stem electrical conductivity measurements. *Soil Sci. Soc. Am. J.* 72, 1014-1024.

Ovington, J. D. (1956), The composition of tree leaves. *Forestry: An international journal of forest research* 29(1), 22-28.

Repo, T., Oksanen, E. & Vappaavuori, E. (2004), Effects of elevated concentrations of ozone and carbon dioxide on the electrical impedance of leaves of silver birch (Betula pendula) clones. *Tree Physiology* 24(7), 833-843.

Rogers, L. E., Beedlow, P. A., Carlile, D. W., & Gano, K. A. (1984), Environmental studies of a 1100-kV prototype transmission line: An annual report for the 1983 study period (Tech. Rep. DOE/BP-371, 1984). https://www.osti.gov/biblio/5926066.

Schubert, E., Sander, J., Ester, M., Kriegel, H. P. & Xu, X. (2017), DBSCAN revisited: Why and how you should (still) use DBSCAN. ACM Transactions on Database Systems 42(3), 1-21.

Sibley, J. T. *The Divine Thunderbolt: Missile of the Gods* (Xlibris US, 2009).

Soula, S., Sauvageot, H., Saissac, M. P. & Chauzy, S. (1995), Observations of thunderstorms by multilevel electric field measurement system and radar. *J. Geophys. Res.* 100(D3), 5025-5035.

Standler, R. B. & Winn, W. P. (1979), Effects of coronae on electric fields beneath thunderstorms. *Q.J.R. Meteorol. Soc.* 105, 285-302.

Toland, R. B. & Vonnegut, B. (1978), Measurement of maximum electric field intensities over water during thunderstorms. *J. Geophys. Res.* 82(3), 438-440.

548 Uman, M. A. (1964), The peak temperature of lightning, *Journal of Atmospheric and Terrestrial*
549 *Physics*, 26, 123-128.

550 Vonnegut, B., Moore, C. B., Stout, G. E., Staggs, D. W., Bullock, J. W. & Bradley, W. E. (1962),
551 Artificial modification of atmospheric space charge. *J. Geophys. Res.* 67(3), 1073-1083.

552 Vonnegut, B. & Rechnitzer, B. W. (1974), Instrument for measuring maximum thunderstorm
553 electric field intensity. *Rev. Sci. Instrum.* 45(9), 1172-1174.

554 Warburg, E. (1899), Spitzenentladung, *Wied. Ann*., *67,* 69-83.

555 Zaffanella, L. E. & Deno, D. W. (1978), Electrostatic and electromagnetic effects of ultrahigh-
556 voltage transmission lines. Final Report (Tech. Rep. EPRI-EL-802, 1978).
557 https://doi.org/10.2172/6650830.

Geophysical Research Letters

Supporting Information for

Corona Discharges glow on Trees under Thunderstorms

P. J. McFarland[1], W. H. Brune[1], D. O. Miller[1] & J. M. Jenkins[1]

[1]Department of Meteorology & Atmospheric Science, The Pennsylvania State University, University Park, PA, 16802

Contents of this file

Additional Supporting Information (Files uploaded separately)

Introduction

There are seven main purposes of this supporting information. First, more information is given on the COTS ultraviolet (UV) camera video processing and filtering (Text S1). Second, more details are presented on the experiments conducted to calibrate the COTS UV camera relative to expected coronae signals and develop the linear relationship to coronae current (Text S2). Third, experiments are discussed that highlight the importance of hydraulic conductance to the coronae current (Text S3). Fourth, one sporadic corona cluster observed on the sweetgum tree during the 27 June 2024 North Carolina case is described in detail (Text S4). Fifth, the sporadic nature of coronae under a constant high-voltage plate is described (Text S5). Sixth, more information is given on the experiments performed that relate coronae UV radiation detected by the COTS UV camera to the total coronae UV emission below 300 nm (Text S6). Finally, experiments conducted with the COMSOL Multiphysics model showcase the importance of leaf orientation on the likelihood of coronae formation (Text S7).

Text S1.

More information on and justification is given here for the thresholds used in the Density Based Spatial Clustering Algorithm with Noise (DBSCAN; Schubert et al., 2017) that distinguishes potential corona clusters. The DBSCAN algorithm identifies clusters of illuminated UV pixels that exceed three carefully chosen thresholds: at least 1 illuminated UV pixel in 4 distinct frames, frames containing illuminated UV pixels are separated by no more than 35 empty frames, or 1.16 seconds, and illuminated pixels only within 10% of diagonal length of the frame of the tree in the corresponding visible video frame are considered. Clusters of illuminated UV pixels that meet or exceed these thresholds are categorized as a potential corona cluster.

These three thresholds were chosen because they maximized the real corona cluster to noise cluster ratio (Fig. S3). To determine this ratio, two COTS UV videos were compared to the same 27 June 2024 North Carolina case visible video. From this visible video, the location of the tree in each frame was determined and compared to any illuminated UV pixels identified in either of the two UV videos. First, the 27 June 2024 North Carolina case UV video was compared, representing the real corona discharge case. Then, a UV video recorded on 8 August 2024, when no thunderstorm was overhead and the COTS UV camera was left capped, was compared to the visible video, representing the noise case.

When UV signals are counted across the entire frame (black line, Fig. S3), the corona-to-noise cluster ratio maximizes at 17 when a maximum of 22 empty frames is permitted between frames with illuminated UV pixels. The first noise cluster is identified when a maximum of 19 empty frames is permitted between frames with illuminated UV pixels, or a frame threshold of 19. Restricting the location of illuminated UV pixels to consider only those near the tree yields several benefits. First, the frame threshold at which the first noise cluster is identified is greatly increased, as no noise clusters are identified for frame thresholds less than 30 when UV signals only within 10% of the diagonal length of the frame from the tree are considered. At 5%, no noise clusters are identified until a frame threshold of 36, thus enabling more confident identification of sparser corona clusters. Second, performing this restriction has a relatively minor impact on artificially removing real corona clusters. About 7% of potential real corona clusters are lost between 100% (black line, Fig. S3) and 10% (teal line, Fig. S3), for frame thresholds less than 35, while 75-100% of noise clusters are lost, offering further confirmation that clusters of UV signals observed under thunderstorms are those from real corona discharges. As further justification for selecting the 10% threshold, the uncertainty in the alignment between the COTS visible and UV camera is estimated to be better than 10%. Thus, UV signals are considered to be associated with the tree if they are within 10% of the frame diagonal length of the tree.

The threshold of four frames with an illuminated UV pixel was similarly chosen to maximize the potential real-corona-to-noise ratio (Fig. S4). For the hour between 19:00 and 20:00 UTC on 27 June 2024, 29 potential corona clusters were identified using the

chosen thresholds. Reducing the required number of frames to contain an illuminated UV pixel from four to three yields 65 potential corona clusters. However, the number of noise clusters identified at this lower threshold skyrockets from 1 to 33, resulting in signal to noise ratios $\leq$ 5 (Fig. S4, black and orange lines). After subtracting off this noise, 32 potential real corona clusters remain. Thus, 10% of potential real corona clusters were lost to filtering as a consequence for removing all the noise. Likewise, increasing the threshold number of frames with an illuminated UV pixel to 5 yields no additional benefits. The first noise cluster is identified at the same frame threshold of 30, and 30% fewer potential real corona clusters are identified. Note that illuminated UV pixels within 10% of the frame diagonal length of the tree were considered for this test.

The final threshold of requiring illuminated pixels to be within 35 frames of each other was chosen for three reasons. First, potential real-corona-to-noise ratios are maximized (Figs. S3-S4). Second, potential coronae signals identified at this threshold are very unlikely to be from noise. Finally, allowing a greater temporal separation between consecutive coronae signals is unphysical, as the likelihood two UV signals are related decreases with time. At a slightly greater frame threshold of 45 (1.5 seconds), 41 potential coronae clusters are found, though at least 5 are likely noise. Thus, restricting the frame threshold to 35 removes all the noise but potentially filters out 20% of potential real coronae clusters. Putting all three filters together removes an estimated 25% of potential real corona clusters.

Text S2.

To relate UV signals recorded by the COTS UV camera to currents, small, potted Spruce and Maple trees were subjected to artificial DC electric fields. A high voltage power supply (Information Unlimited HV350REG) that outputs $\pm$5 to $\pm$35 kV charged a 66 cm by 61 cm aluminum plate 15 cm above treetop. A grounded metal ring encircled a lower portion of the tree, typically 70 cm below the charged aluminum plate. A picoammeter (Keithley 6485) measured the current flowing between a copper plate in the soil beneath the tree roots and an earth ground. Several voltages up to $\pm$30 kV were supplied to the aluminum plate and held constant for at least 60 seconds while the COTS UV camera recorded UV signals 12 m away.

Average COTS UV camera signals in illuminated pixels s^{-1} scaled linearly with current flowing through the tree (Fig. S6). Lowering the separation between the charged aluminum plate and treetop to 10 cm increased current flow by a factor of 2 in the spruce tree and 5 in the maple tree, though average COTS UV signals increased proportionally. Decreasing the separation between the charged aluminum plate and grounded metal ring by a factor of two had negligible impacts on the current or UV signals. Thus, the UV signal to current relationship is found to be robust, holding over

several orders of magnitude, and independent of electric field and tree type. From UV signals recorded by the COTS UV camera, estimates of current are possible.

The factor with the greatest influence on the COTS UV signal to current relationship is corona polarity. While absolute values of the currents are similar between the two corona polarities, UV signals recorded by the COTS UV camera were an average factor of 2.5 greater in negative coronae than in positive. This difference is a result of the mechanisms that sustain positive and negative corona discharges. When the overhead aluminum plate is negatively charged, a negative current is measured through the soil, and a positive charge is induced in the tree. Positively polarized coronae are sustained primary through photoionization, a process by which neutral atoms emit electrons after absorbing a high-energy photon, and appear as elongated, streamer-like structures (Dordizadeh et al., 2016; Luque er al., 2008; Jenkins et al., 2022). Conversely, negative coronae are sustained primary through impact ionization, where high-energy electrons collide with neutral molecules that subsequently eject a new electron, and appear as point discharges (Dordizadeh et al., 2016; Luque et al., 2008; Jenkins et al., 2022). Negative coronae contain a greater number of electrons (Chen & Davidson, 2002; Luque et al., 2008) and therefore emit stronger UV radiation, explaining the larger average COTS UV signal rates observed from negative coronae (Fig. S6).

The COTS UV camera recorded UV signals at least a factor of two above the background noise for electric field magnitudes greater than 20 kV m^{-1}, nearly identical to those measured at altitudes typical of and above mature ~20 m-tall trees (Standler & Winn, 1979; Soula et al., 1995; Chauzy & Raizonville, 1982). Thus, there is unlikely to be a multitude of weaker coronae on trees under thunderstorms below the COTS detection threshold.

Text S3.

The small Maple tree used in the experiments to relate COTS UV signals to current was dug up from one of the authors' backyards, severing the main roots in the process. Thus, the Maple tree began dying, providing an opportunity to test current flow through a tree with decreasing hydraulic conductance. Such experiments were performed approximately weekly for three weeks, 1, 6, and 13 days after being dug up, using the experimental setup described above in Text S2.

Current flow through the tree was greatest on day 1, measuring 3.86 μA when the overhead aluminum plate was charged to 18.9 kV (Fig. S7a). On day 6, the current measured at 18.9 kV decreased to 1.24 μA, a factor of 3.1 decrease. Current decreased to 0.8 μA, a further factor of ~1.6, on day 13, by which point the leaves were beginning to sag and turn brown. The tree was kept well-watered throughout these three weeks, and water was always applied to the soil just prior to these voltage-current experiments. Therefore, the observed decrease in current is most likely attributable to the decrease in hydraulic conductance as the tree died, supporting the findings of previous studies

(Ganthaler et al., 2019; Nadler et al., 2008; Bucci et al., 2003; Flexas et al., 2003; Afzal et al., 2017; Mancuso 1999).

Despite the decaying voltage-current relationship, observed COTS UV signals remained linearly proportional to current (Fig. S7b). On day 1, COTS UV signals averaged 68.8 illuminated pixels s^{-1} for a voltage of 18.9 kV. At the same voltage on day 6, the average COTS UV signal was 26.9 illuminated pixels s^{-1}, a factor of 2.6 decrease, similar to the factor of 3.1 drop in current. Likewise, average COTS UV signals dropped by an additional factor of 1.1 to 24.2 illuminated pixels s^{-1} on day 13. Thus, the COTS UV signal to current relationship is independent of hydraulic conductance in addition to electric field and tree type (See Text S2).

Text S4.

The behavior of coronae on tree leaves under thunderstorms is illustrated by one example corona that persisted for 2.76 seconds on the sweetgum tree observed on 27 June 2024 (Fig. S9). In those 2.76 seconds, wind blew the branch across much of the field of view (Movie S1) and heavy rain rates exceeding 32 mm hr^{-1} scattered the corona UV signal such that pinpointing the exact position of the corona on a leaf is difficult. Six unique UV signals comprise this corona cluster, observed in six of 83 frames and are numbered in their order of observation in Fig. S9. The first UV signal in this corona cluster occurred in the upper right corner of the frame, followed 28 frames (~1 s) later by a rapid succession of three corona UV signals in three consecutive frames coming from three different leaves at points 2, 3 and 4. In these three frames, the corona hopped from the top of the middle branch (Point 2) to the bottom left portion of the middle branch (Point 3) to the upper edge of the leftmost branch (Point 4), whose edge comprises the bottom left corner of the COTS UV camera field of view at this time. The corona UV signal at point 5 was observed two frames after point 4 and hops back to the middle branch from the rightmost branch, near the location of the third signal. The final UV signal at point 6 occurred eighteen frames after point 5, in nearly the same location.

These UV signals could be from individual, discreet coronae that exist for just one frame (33 ms) or a single corona that lasts for a few seconds. No attempt is made here to distinguish between the two, as the clustering was made strictly for filtering out noise. Regardless, these observed coronae on this one branch are sporadic and short-lived, hopping from leaf to leaf, branch to branch, and sometimes coming back to the same leaf.

Text S5.

The behavior of coronae on trees under thunderstorms was observed to be sporadic, hopping from leaf to leaf and branch to branch while occasionally returning to a leaf (See Main Text Section 3; Text S4; Fig. S9). To determine if a similar behavior is observed in the laboratory with a constant overhead voltage, we examine the coronae

recorded when a -15.8 kV voltage (-20.5 kV m^{-1}) was applied to the fresh Maple tree using the experimental setup described in Text S2.

Five distinct coronae were observed (Fig. S10a). Four of the five were along the top leaf canopy, while the last was on a slightly lower leaf that extended towards the camera, and was unshielded from the electric field by the upper canopy. The remainder of the lower leaves did not record any repeated UV signals, likely because they were shielded from experiencing the overhead electric field by the coronae along the top leaves. The strongest corona formed on the leaf closest to the overhead aluminum plate (orange box; Fig. S10a) while the weakest was on the opposite end of the top canopy (blue box; Fig. S10a).

For all five coronae, UV signals were observed to be sporadic (Fig. S10b). The strongest corona is also the most consistent (orange line, Fig. S10b), though there are several instances of several frames without any UV signal for this corona. For instance, no UV signals were recorded for this strongest corona between frames 691 and 736, a duration of 1.5 seconds. At the same time, the corona enclosed by a pink box, just to the left of the strongest, experienced its greatest density of UV emission. Likewise, the lower corona enclosed by a yellow box emitted its strongest UV signal during this period. The corona jumped from its preferred location to two other, less preferred locations, before returning to its initial location, just as observed on trees under thunderstorms.

Another example of similar behavior is seen between frames 918 and 1437, a duration of 17.3 seconds. Here, no UV signals were recorded for the corona enclosed by the purple box. Rather, the weakest, blue-boxed corona just to the left experienced its greatest UV signal density. The corona again jumped from the more-preferred, purple-boxed location to the less-preferred, blue-boxed location before returning. Thus, coronae are sporadic and jumpy in nature, even under a constant high voltage. Such behavior is only expected to exacerbate on trees under a highly heterogeneous electric field

Text S6.

To relate the coronae UV emission detected by the COTS UV camera to the total coronae UV emission below 300 nm, the wavelengths capable of producing OH by dissociating water (H_2O) and ozone (O_3), the coronae spectrum was measured using a spectrometer (Ocean Optics Ocean HR). The spectrometer is sensitive to wavelengths of ~195 nm to 850 nm. Two different coronae tests were performed. First, a corona discharge on a copper rod beneath a charged aluminum plate was measured. Second, a corona discharge was initiated the laboratory flow tube setup described by Jenkins et al. (2021). Using the same deuterium lamp as in the COTS calibration (StellarNet SL3), the transmissivity of the spectrometer was calibrated, and the coronae spectrum was corrected accordingly. In both cases, total coronae UV emission between 195 and 300

nm was about a factor of seven greater than the UV emission between 255-273 nm, the full width half maximum of the COTS UV camera.

Text S7.

To simulate the importance of leaf orientation on coronae formation, a locust stem containing several leaves was inserted horizontally 4.4 cm below a plate charged to 14 kV in a COMSOL Multiphysics simulation, like the laboratory experiments of Jenkins et al (2022). When the leaves and their sharp points were oriented toward the high voltage plate, the local electric field was enhanced beyond the breakdown electric field necessary for corona discharge formation on every leaf (Fig. S11a). Conversely, when the leaves were oriented away from the high voltage plate, no enhancements capable of producing coronae were found (Fig. S11b). Therefore, leaf orientation is a critical factor that modulates local electric field enhancement and coronae formation. As the wind constantly reorients leaves on a tree, those capable of forming coronae constantly change.

Figure S1. The COTS storm-intercept research vehicle (2013 Toyota Sienna). Light enters the optical pathway through a (a) 30.5-cm window in the periscope, where it is directed down into the vehicle by two ¼-wave flat turning mirrors. A small pickoff mirror directs some of this light to (b) the OFiL camera, a wider field-of-view, less sensitive version of the COTS UV camera, while the rest enters (c) a 25-cm diameter f4.0 Newtonian telescope, where it is focused into (d) the COTS visible and UV cameras. The system is powered by a battery and data are stored on either a digital video recorder or (e) a laptop hard drive. (f) The electric field mill measures the uncalibrated electric field

relative to the roof of the vehicle, while (g) a weather station measures meteorological variables including pressure, temperature, and rainfall.

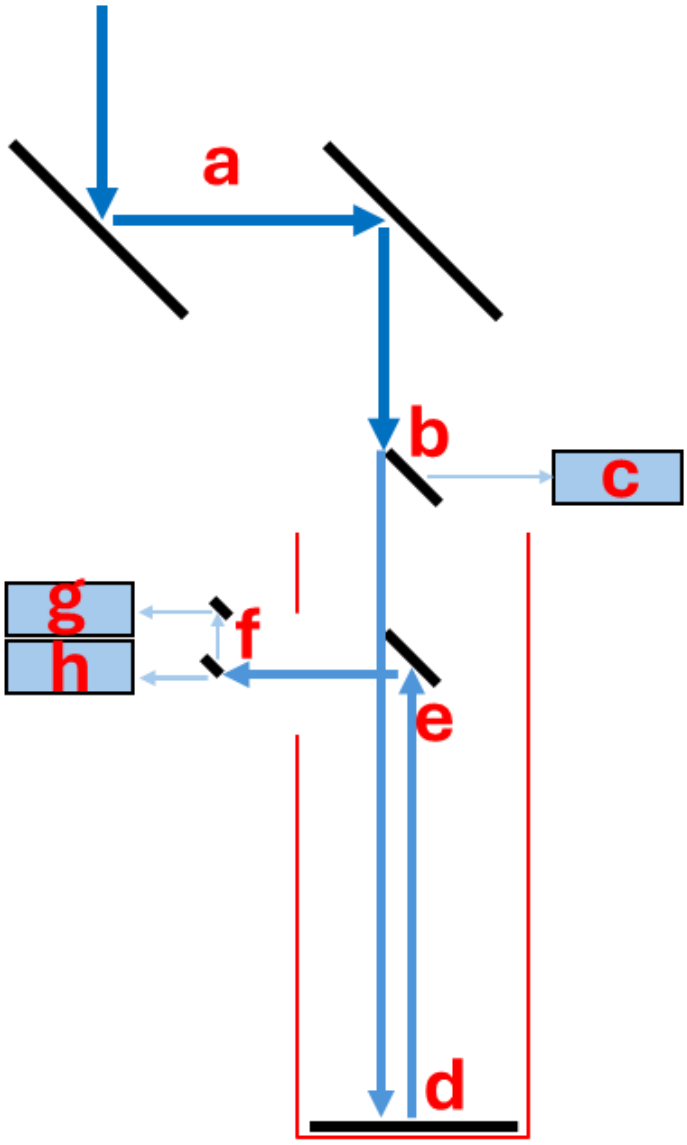

Figure S2. Diagram of the optical arrangement of the COTS instrument. Light (blue arrows) enters the system through a 30.5-cm diameter 0.05-mm thick Teflon FEP window on the periscope and is directed down into the vehicle by (a) two λ/4 flat turning mirrors (Precision Optical). (b) A small flat turning mirror directs some of this light to (c) the OFiL camera, a wider field-of-view, less sensitive version of the COTS UV camera, while the rest enters a 25-cm diameter f4 Newtonian telescope (red outline). (d) The primary telescope mirror focuses light onto (e) a secondary flat turning mirror which directs light out of the telescope. (f) A small, 1.3-cm by 1.3-cm flat turning mirror picks off some light to send to (g) a visible camera while the remaining light is focused on (h) the COTS UV camera.

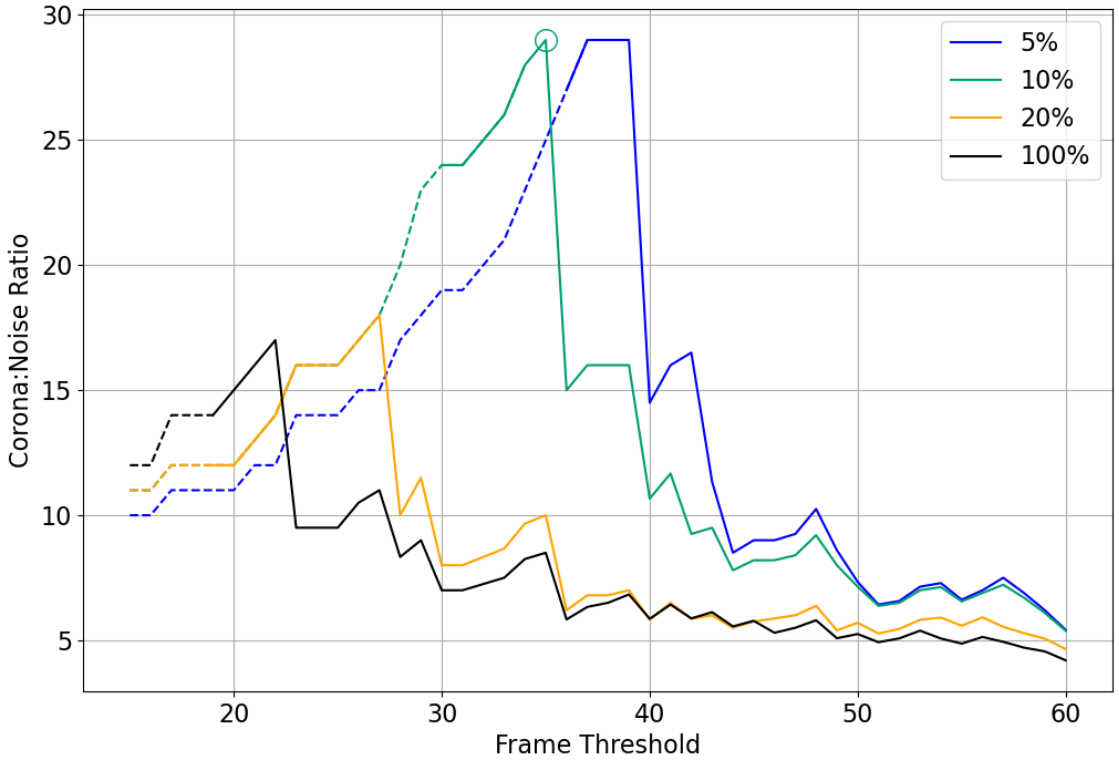

Figure S3. Ratio between the number of potential real corona clusters and noise clusters identified by the DBSCAN processing algorithm for varying thresholds. The x axis denotes the maximum number of empty frames devoid of UV signal permitted between frames with illuminated UV pixels for them to be clustered together. Colors denote the percentage of the frame diagonal length beyond the tree edge for which UV signals were kept. Dashed lines correspond to the number of corona clusters identified by the DBSCAN algorithm for which no noise clusters were identified. The teal circle denotes the selected thresholds of 10% of the frame diagonal length and a maximum of 35 frames,

or 1.16 seconds, between consecutive frames with an illuminated UV pixel used in this study.

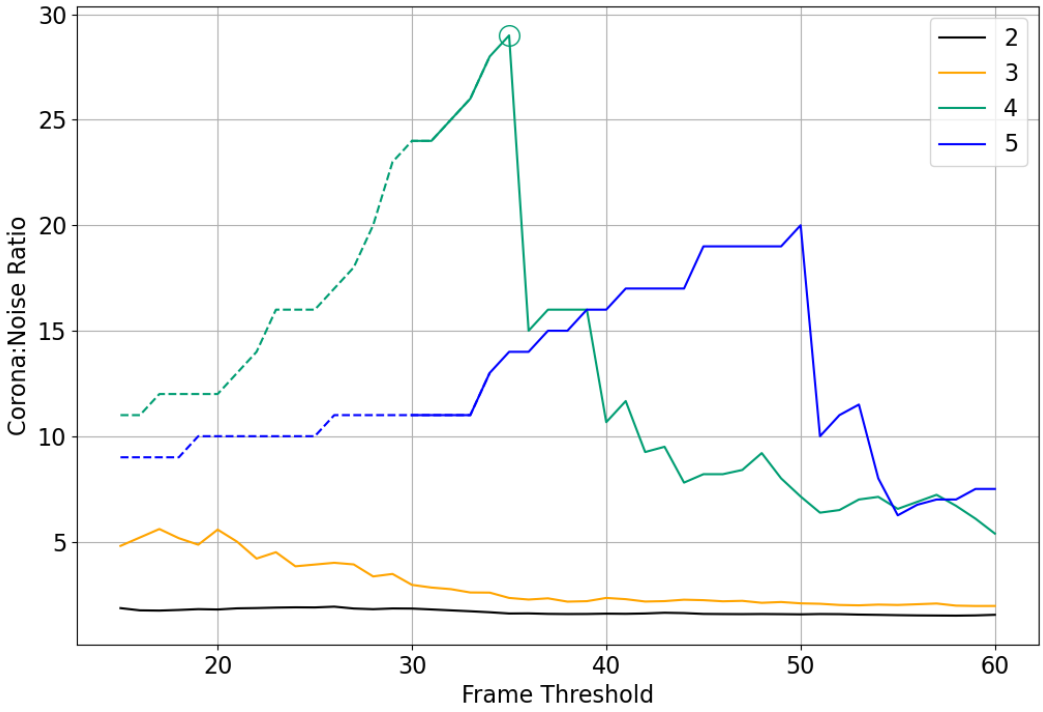

Figure S4. Ratio between the number of potential real corona clusters and noise clusters identified by the DBSCAN processing algorithm for varying thresholds. The x axis denotes the number of empty frames devoid of UV signals permitted between illuminated UV signals for them to be clustered together. Colors denote the number of frames that must contain an illuminated UV pixel for a cluster to be identified. Dashed lines correspond to the number of corona clusters identified by DBSCAN for which no noise clusters were identified. The teal circle denotes the selected thresholds of four frames with an illuminated UV pixel separated by no more than 35 frames, or 1.16 seconds, used in this study.

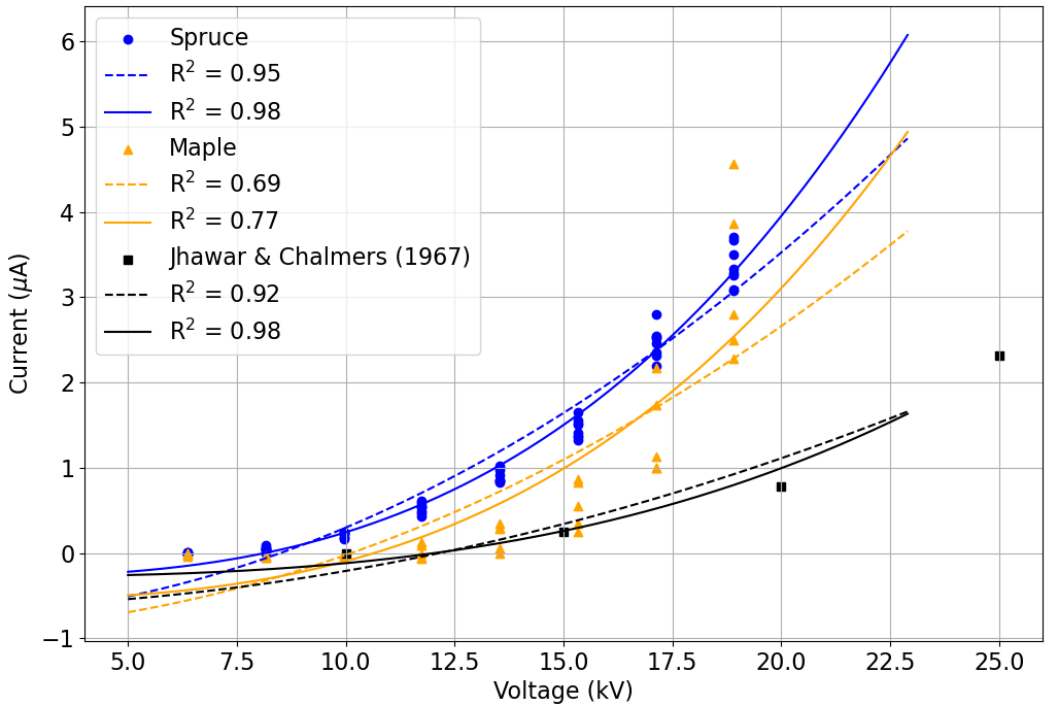

Figure S5. Applied voltage vs. measured current curves for the tested Spruce (blue) and Maple (orange) trees under a positively charged aluminum plate. A quadratic fit is given by the dashed lines while a cubic fit is given by the solid lines. Similar relationships and fits were obtained when the aluminum plate was negatively charged. Also included is the relationship between applied voltage and measured current found by Jhawar & Chalmers (1967) experiments with a heavily trimmed spruce tree (black).

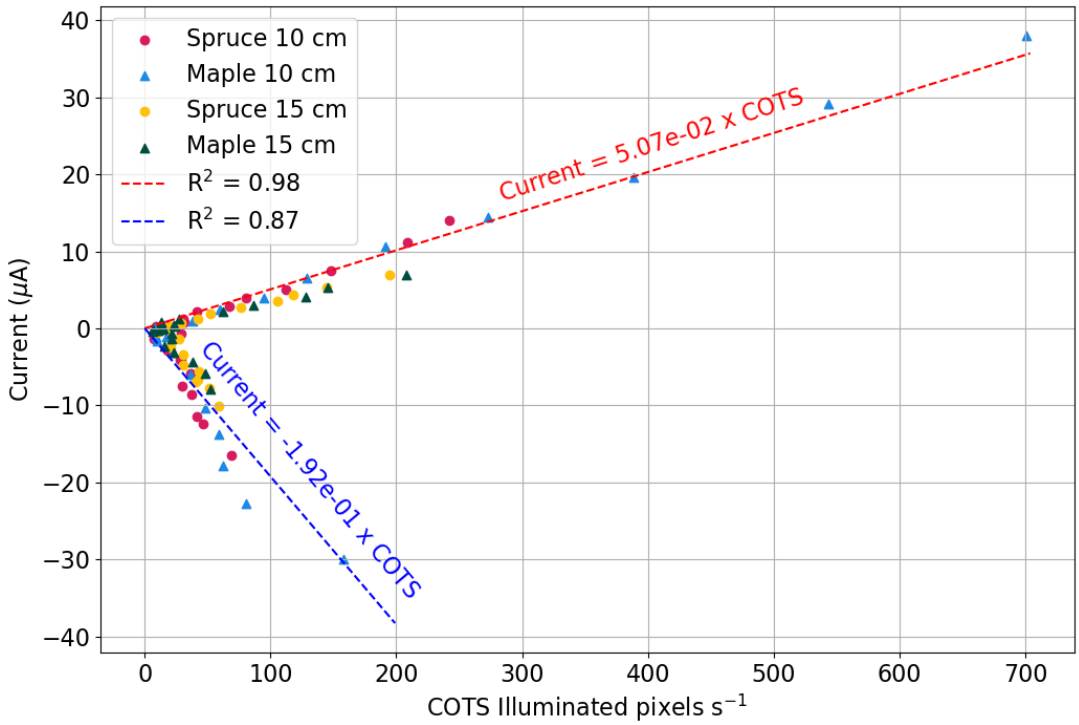

Figure S6. COTS UV camera signals (illuminated pixels s^{-1}) against current measured in the soil beneath the tree roots by a picoammeter. Both a Spruce and Maple tree were placed 10 to 15 cm below a charged aluminum plate. When the plate was positively charged and the tree grounded, positive currents were measured. COTS UV signals scaled linearly with current with a slope of 5.07×10^{-2} μA s $pixel^{-1}$ and an R^2 of 0.98. When the plate was negatively charged and the tree grounded, a negative current was

measured. COTS UV signals scaled linearly with current with a slope of -0.192 μA s pixel^{-1} and an R^2 of 0.87.

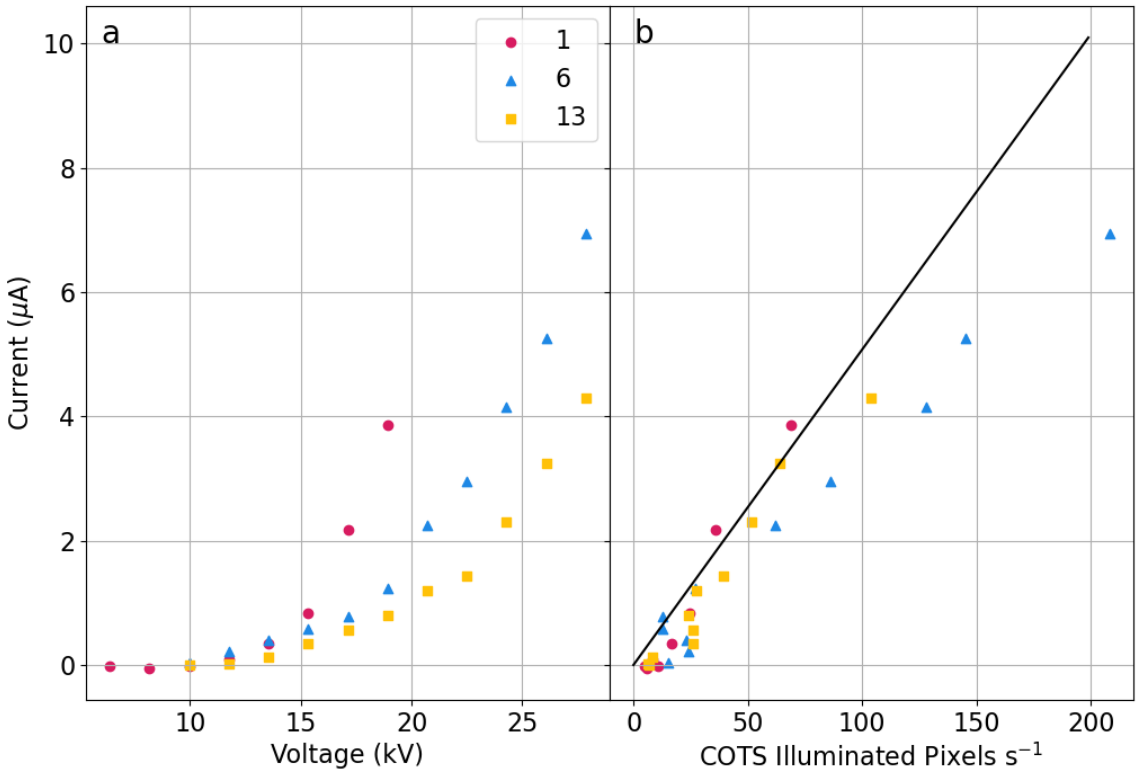

Figure S7. Hydraulic conductance to current experiments. The Maple tree was tested three times on three different days as it died, 1 (red circles), 6 (blue triangles), and 13 (yellow squares) days after its roots were severed. (a) The voltage to current slope decayed as the tree died and hydraulic conductance decreased. (b) The slope of the COTS illuminated pixels vs current line did not change much and remained closely scattered around the fit line defined in Figure S6 for negative coronae. A similar relationship was found for positive coronae.

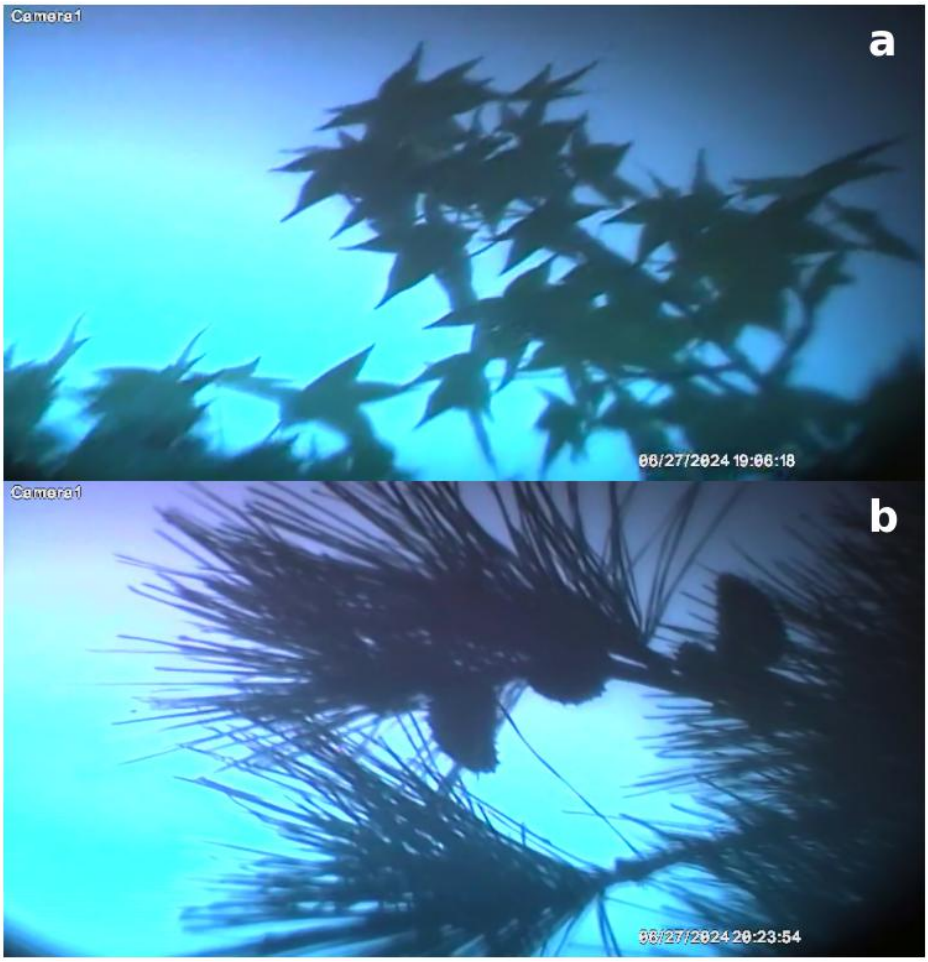

Figure S8. Example frames from the COTS visible camera of (a) the sweetgum tree, and (b) the loblolly pine tree examined for ~1.5 hours and ~20 minutes under a thunderstorm on 27 June 2024. Sweetgum leaves contain five distinct sharp points in a star-like pattern. Conversely, loblolly pine leaves are long (~15 cm) and thin and end in a fine tip. A few seed cones are also visible on the loblolly pine tree.

Figure S9. Six corona discharge UV signals observed during a 2.76 second period from 19:19:59 to 19:20:01 UTC on a sweetgum tree in Pembroke, NC on 27 June 2024. UV signals detected by the COTS UV camera are expanded, numbered by order of occurrence, and overlaid on the COTS visible camera closest to the location on the leaves where the signal occurred considering the leaves were moved across the frame by the wind (See Movie S1).

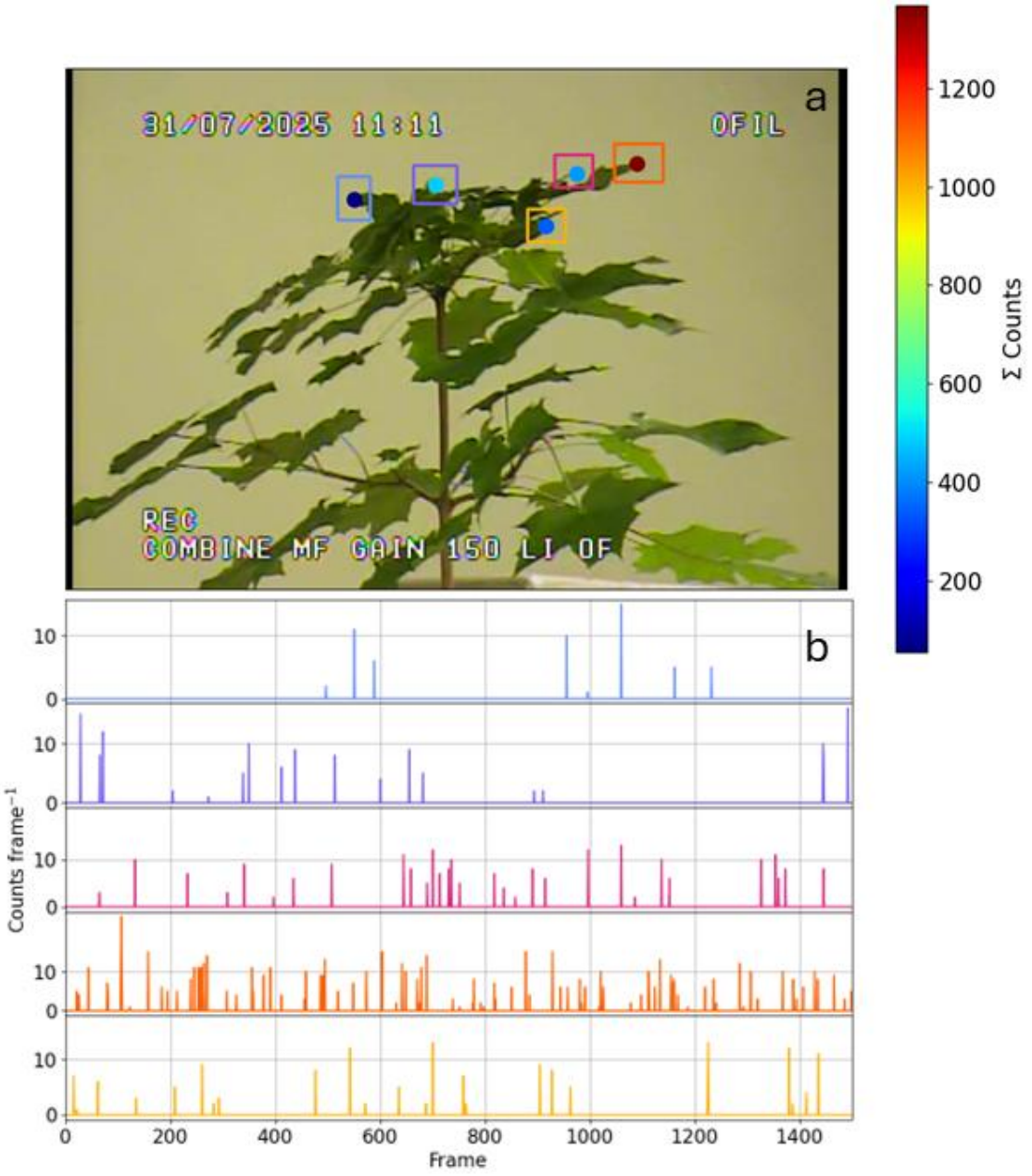

Figure S10. Five coronae locations observed when the Maple tree was 15 cm below the aluminum plate charged to -16 kV. The five coronae locations are boxed in (a), with the color of the box corresponding to the timeseries of counts observed for that corona cluster in (b). Across the top of the tree from left to right, the blue, purple, pink, and orange boxes correspond to time series rows 1-4. The yellow box around the corona below the top branches corresponds to the bottom timeseries. Each corona location in (a) is colored by the sum of counts (illuminated pixels) observed in that corona cluster over the one minute for which the experiment was performed.

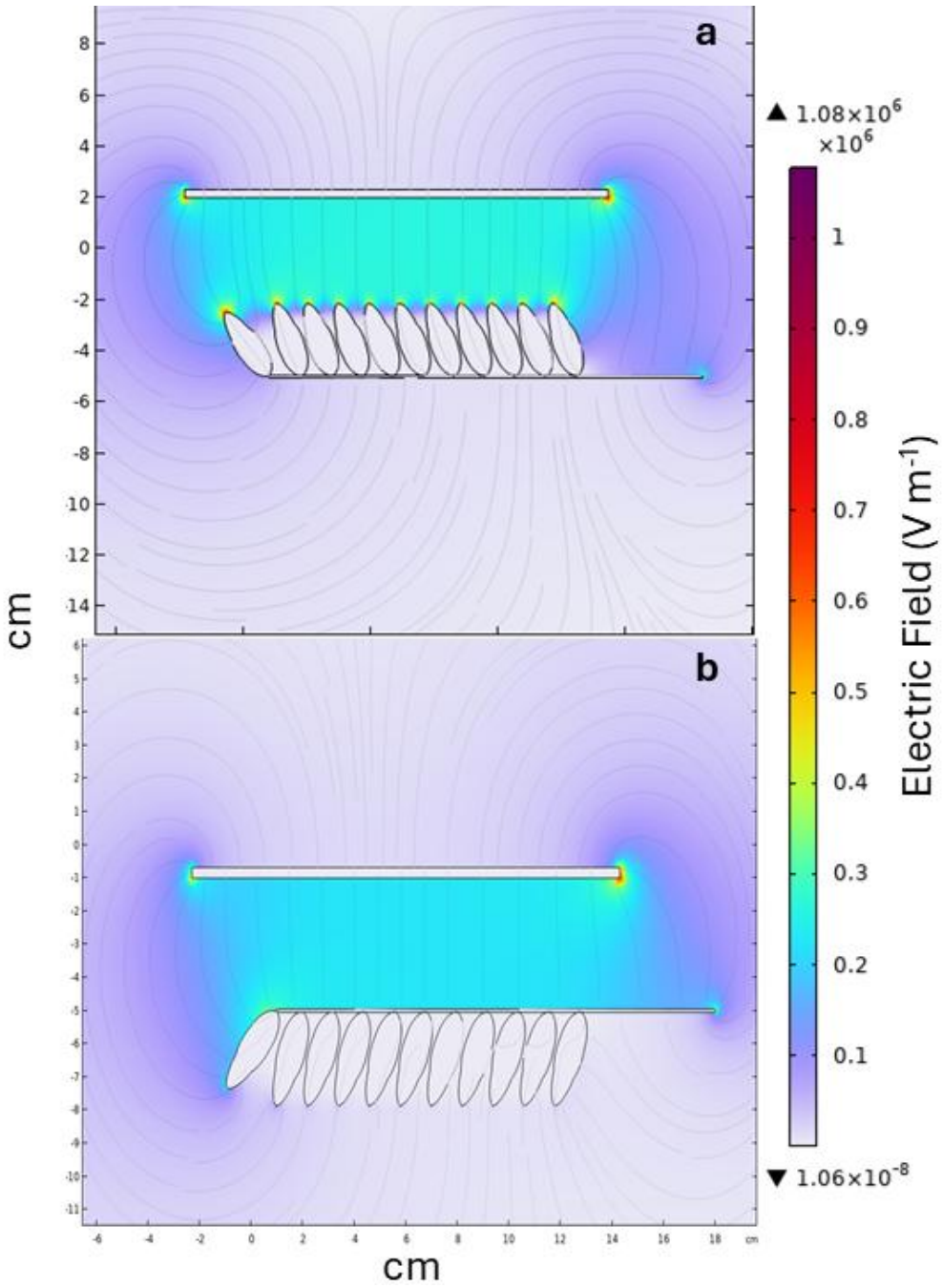

Figure S11. COMSOL Multiphysics simulations demonstrating the importance of leaf orientation on coronae formation. In (a), the sharp points of the locust stem leaves were oriented towards the charged plate, and electric field enhancements capable of producing coronae were found on all leaves. Conversely, in (b), the sharp points were turned away from the charged plate and no locations were found to have electric fields large enough to support coronae formation.

Date	**Time (UTC)**	**Location**	**Tree**	**Intensity (10^{11} ph frame^{-1})**	**Current (μA)**
2024-06-25	00:24:36 – 01:45:00	-81.9793°E, 28.0295°N	Live Oak	8.9 (4.5)	2.0 (1.0)
2024-06-27	18:44:45 – 20:05:20	-79.1981°E, 34.6989°N	Sweetgum	25 (17)	4.1 (0.8)
2024-06-27	20:10:20 – 20:34:09	-79.1983°E, 34.6986°N	Loblolly Pine	3.3 (1.7)	1.1 (0.8)
2024-07-30	19:54:40 – 20:29:26	-77.8901°E, 40.7742°N	Pin Oak	6.2 (3.9)	2.4 (2.5)
2024-07-30	20:29:46 – 21:00:54	-77.8901°E, 40.7742°N	Spruce	11 (4.3)	3.6 (1.3)
2024-08-06	19:26:48 – 20:21:39	-77.8279°E, 40.8212°N	Tulip	7.9 (2.8)	3.6 (2.0)
2024-08-18	00:19:48 – 02:05:20	-77.8943°E, 40.7165°N	Pin Oak	5.4 (2.9)	1.2 (0.9)

Table S1. Cases observing coronae on trees under thunderstorms. The time spans the duration for which the COTS was operating under a thunderstorm at the given location observing the given tree type, while the intensity is the mean (median) photon emission rate from observed corona UV signals, and the current is the mean (median) absolute value of the coronae current estimated from the observed coronae signals.

Movie S1. Video of the COTS UV signals observed for the corona shown in Fig. S9. The corona contains 6 frames with distinct UV signals over 2.76 seconds between 19:19:59 and 19:20:01 UTC.